

Figure 1—Intraoral photograph of the left parotid papilla of a 10-year-old 7-kg (15.4-lb) Chihuahua cross that was evaluated because of recurrent left-sided facial swelling and purulent discharge from the oral cavity. The papilla was slightly erythematous and more prominent than that on the right side.

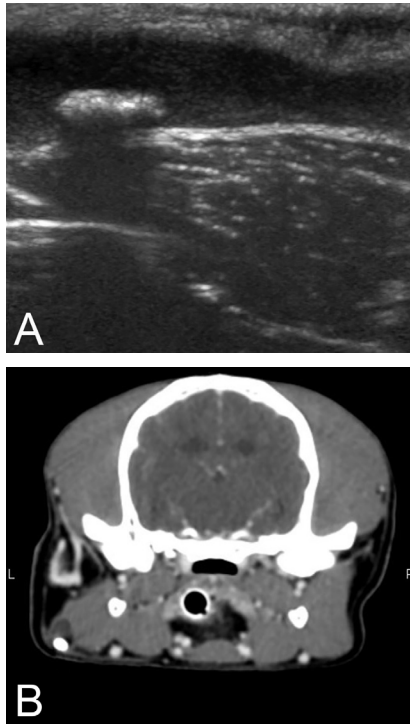


Figure 2—Ultrasonographic (A) and contrast-enhanced CT (B) images obtained from the same dog as in Figure 1. The ultrasonographic image (parasagittal view) was obtained over the region of facial swelling by use of a ventral approach with the animal in dorsal recumbency. The transverse CT image of the skull (slice thickness, 0.6 mm) was obtained at the level of the first maxillary molar teeth and viewed with bone (window width, 2,500 Hounsfield units [HU]; window level, 480 HU) and soft tissue (window width, 750 HU; window level, 200 HU) window settings. L = Left. R = Right.

History and Physical Examination Findings

A 10-year-old 7-kg (15.4-lb) spayed female Chihuahua cross was referred to a veterinary teaching hospital because of recurrent left-sided facial swelling and purulent discharge from the oral cavity. The client had noticed an increase in lip smacking and licking approximately 6 months prior to the evaluation. Facial swelling and signs of pain on palpation had first been detected 10 weeks prior to the examination; the dog had been treated by the referring veterinarian for a suspected tooth root abscess or abscess secondary to a foreign body. An antimicrobial (amoxicillin trihydrate–clavulanate potassium; 18 mg/kg [8.2 mg/lb], PO, q 12 h for 14 days) and an NSAID (carprofen; 1.8 mg/kg [0.82 mg/lb], PO, q 12 h for 7 days) had been prescribed. Clinical signs had improved over the course of initial treatment but relapsed following cessation of the treatment. The referring veterinarian anesthetized the dog, obtained intraoral dental radiographs, and performed periodontal charting. Mild to moderate localized periodontitis was diagnosed with no evidence of a dentoalveolar abscess or dental cause for the facial swelling.

On examination at the referral visit, the dog was bright, alert, and responsive with no abnormalities found on general physical examination other than a fluctuating soft tissue swelling in the region over the left masseter muscle. Intraoral examination revealed a prominent, erythematous left parotid papilla (**Figure 1**), concurrent sialorrhea upon digital manipulation of the ipsilateral parotid gland, hypodontia, and mild generalized plaque and calculus accumulation. Blood and urine samples were obtained for a CBC, serum biochemical analysis, and urinalysis. Laboratory test results were unremarkable.

The dog was sedated with dexmedetomidine hydrochloride (3.0 µg/kg [1.36 µg/lb], IV) and butorphanol tartrate (0.1 mg/kg [0.045 mg/lb], IV), and ultrasonographic evaluation of the swollen facial region was performed; the following day, the dog was anesthetized, and contiguous transverse collimated CT images of the skull were obtained at a slice thickness of 0.6 mm before and after IV contrast medium administration (**Figure 2**). The images were viewed with bone (window width, 2,500 Hounsfield units [HU]; window level, 480 HU) and soft tissue (window width, 750 HU; window level, 200 HU) settings. Three-dimensional volume rendering was performed, and all digital images were reviewed on a medical-grade flat screen monitor, by use of commercially available software.⁴

Determine whether additional studies are required, or make your diagnosis, then turn the page→

This report was submitted by Peter C. Strøm, DVM; Daniel S. Bucy, DVM; and Boaz Arzi, DVM; from the Dentistry and Oral Surgery Service, William R. Pritchard Veterinary Medical Teaching Hospital (Strøm, Bucy), and the Department of Surgical and Radiological Sciences (Arzi), School of Veterinary Medicine, University of California–Davis, Davis, CA 95616.

Address correspondence to Dr. Arzi (barzi@ucdavis.edu).

Diagnostic Imaging Findings and Interpretation

Ultrasonographic imaging revealed a markedly dilated and mildly echogenic fluid-filled left parotid salivary duct with a hyperechoic epithelial lining. A discrete, hyperechoic shadowing structure, consistent with mineralized material, was visualized at the mid portion of the duct (**Figure 3**). The structure was spherocylindrical and freely movable and measured $8 \times 4 \times 3$ mm. The duct was dilated rostral and caudal to the hyperechoic structure. The left parotid salivary gland was mildly enlarged and slightly

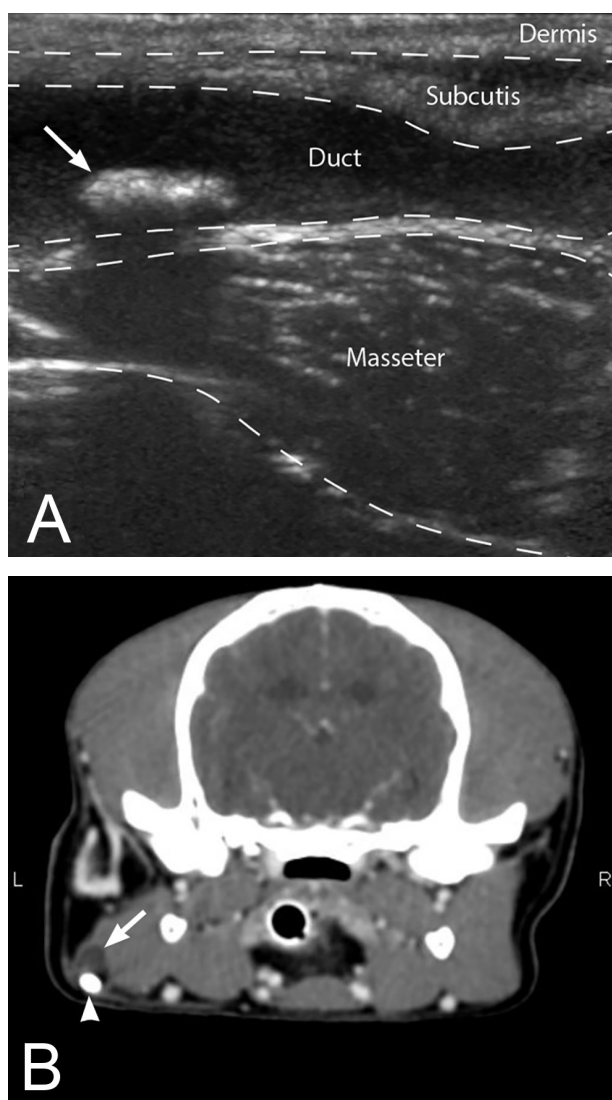


Figure 3—Same diagnostic images as in Figure 2. In the ultrasonographic image (A), notice the dilated and echogenic fluid-filled left parotid salivary duct superficial to the masseter muscle. There is a spherocylindrical hyperechoic structure within the ductal lumen, consistent with a sialolith (arrow). In the transverse CT image of the skull (B), a dilatation of the left parotid salivary duct with a fluid-attenuating lumen (arrow) is evident, and a homogeneous, ovoid, smoothly margined mineral-attenuating structure is present within the duct (arrowhead) See Figure 2 for remainder of key.

hypoechoic, compared with the contralateral parotid gland, suggesting possible sialoadenitis. A sialolith with secondary sialoadenitis was tentatively diagnosed.

On CT examination, a marked fluid-attenuating dilatation of the left parotid duct, extending from the parotid gland to the parotid papilla, was observed (**Figure 3**). The ductal wall appeared mildly thickened and was peripherally contrast enhancing. A smooth, spherocylindrical, approximately $8 \times 4 \times 3$ -mm mineral-attenuating structure was evident within the left parotid duct on collimated transverse and 3-D CT images. The left mandibular lymph node was slightly enlarged, compared with that on the right, and was mildly and heterogeneously contrast enhancing. An unerupted right mandibular first premolar tooth was identified as an incidental finding on CT images.

Treatment and Outcome

A left infraorbital nerve block was performed with bupivacaine hydrochloride (0.4 mL of a 5 mg/mL solution; 0.29 mg/kg [0.13 mg/lb]), and supragingival sonic scaling was performed. Ultrasonography was used intraoperatively, directly following CT, to locate the movable sialolith within the parotid salivary duct and allow for easier extirpation. A transoral approach was used for sialolithectomy, and a stoma of the salivary duct was created by everting the ductal epithelium and suturing it to the mucosal lining with 5-0 poliglecaprone-25 suture material. Ampicillin sodium (20 mg/kg [9.1 mg/lb], IV) was administered intraoperatively.

The dog received hydromorphone hydrochloride (0.05 mg/kg [0.023 mg/lb], IM) once and meloxicam (0.1 mg/kg, IV) once after surgery. Following routine recovery, the dog was discharged from the hospital with tramadol hydrochloride (1.8 mg/kg [0.82 mg/lb], PO, q 8 to 12 h), amoxicillin trihydrate-clavulanate potassium (17.8 mg/kg [8.1 mg/lb], PO, q 12 h), meloxicam (0.1 mg/kg, PO, q 24 h for 7 days), and a 0.12% chlorhexidine gluconate oral rinse to be used once every 8 to 12 hours for 2 weeks. Ultrasonography was performed 15 days after surgery to evaluate the echogenicity of the glandular parenchyma and dilatation of the ductal system and to verify that the stoma created was functional. Oral examination revealed a healing incisional site with no palpable swelling and a patent stoma. Ultrasonographic evaluation subjectively normal glandular parenchyma with no dilatation of the parotid duct.

Comments

Several possible explanations have been proposed for the etiopathogenesis of sialolith formation in people and dogs, including inflammatory processes,¹ the excretion of microcalculi by acinar cells, or the presence of intraluminal mucous plugs.² Retrograde bacterial migration with secondary inflammation can possibly create an organic nidus for deposi-

tion of inorganic components.^{1,2} Furthermore, it has been reported that foreign bodies such as a fragment of a wooden toothpick or grass awn can migrate into a salivary duct and lead to sialolith formation in people,^{2,3} and this could also happen in dogs.

Clinical signs of this disease in dogs usually include an acute to chronic unilateral facial swelling in the region of the affected salivary gland and a tubular tumescent cystic region lateral to the masseter muscle, likely resulting from ductal dilatation and sialorrhea, with or without signs of oral pain. In addition, purulent fluids may be seen in the oral cavity,³ and ductal rupture can sometimes occur.⁴ There is often no known history of trauma, and the swelling may resolve and recur over several months in correspondence to empirical treatment with antimicrobials, anti-inflammatory drugs, or corticosteroids. This makes the condition difficult to diagnose on the basis of clinical signs alone, and it could be confused with a periocular swelling secondary to a dentoalveolar abscess or foreign body. Factors such as the location of the facial swelling and the size and skull conformation of the dog of this report could further contribute to the condition being mistaken for a dentoalveolar abscess.

A definitive diagnosis and treatment plan may require more than 1 diagnostic modality to accommodate for the shortcomings of individual methods. Conventional radiography, sialography, and CT³ are commonly used diagnostic imaging techniques in veterinary dental practices. In human patients, ultrasonography has been used and, more recently, sialoendoscopy has emerged as a minimally invasive diagnostic and treatment modality for sialolithiasis.⁵

Dreiseidler et al⁶ suggested that conventional radiographic images have limited success in identifying sialoliths because of overlapping anatomic structures. Moreover, Som and Curtin⁷ estimated that 20% of submandibular salivary gland sialoliths and 40% of parotid gland sialoliths are missed on plain radiographic images because of low calcium content, and this is not considered the preferred method of diagnosing sialoliths in people. Ultrasonography is a radiation-free alternative with 77% sensitivity and 95% specificity for the detection of calculi in human patients with sialolithiasis.⁸ Computed tomography was found to be more accurate for identification of submandibular salivary gland sialoliths in people, compared with conventional radiography and ultrasonography⁹; it also allows simultaneous evaluation of the parotid salivary duct and gland. For the dog of this report, a decision was made to perform ultrasonography and CT. The critical information that the sialolith was freely movable within the duct would not have been available

if only a CT scan was performed, and alternatively, a different (extraoral) surgical approach might have been elected.

Marked dilatation of the parotid duct was apparent at the time of surgery in this patient, and although previous inflammation and possibly infection of the parotid gland were present, it was decided to reconstruct the duct and create a new stoma. In this patient, as in previous reports,^{5,10} the choice of treatment produced a successful outcome.

Ultrasonography and CT proved to be important in diagnosing sialoadenitis secondary to sialolith formation and for surgical planning for the dog of this report. Specifically, determining that the stone was freely movable within the duct led to the determination that the sialolith could be removed through a transoral approach. This case exemplifies the value of advanced diagnostic imaging when assessing orofacial swelling of unknown origin. Likewise, a comprehensive pertinent history and oral and physical examination are crucial to appropriately identify and localize the disease, select the proper diagnostic tools, and determine a treatment plan.

Footnotes

- a. eFilm, eFilm Workstation, version 2.1.0, Merge Healthcare, Chicago, Ill.

References

1. Harvey CE. Sialography in the dog. *Vet Radiol Ultrasound* 1969;10:18-27.
2. Marchal F, Kurt AM, Dulguerov P, et al. Retrograde theory in sialolithiasis formation. *Arch Otolaryngol Head Neck Surg* 2001;127:66-68.
3. Trumpatori BJ, Geissler K, Mathews KG. Parotid duct sialolithiasis in a dog. *J Am Anim Hosp Assoc* 2007;43:45-51.
4. Termote S. Parotid salivary duct mucocele and sialolithiasis following parotid duct transposition. *J Small Anim Pract* 2003;44:21-23.
5. Kiringoda R, Eisele DW, Chang OL. A comparison of parotid imaging characteristics and sialendoscopic findings in obstructive salivary disorders. *Laryngoscope* 2014;124:2696-2701.
6. Dreiseidler T, Ritter L, Rothamel D, et al. Salivary calculus diagnosis with 3-dimensional cone-beam computed tomography. *Oral Surg Oral Med Oral Pathol Oral Radiol Endod* 2010;110:94-100.
7. Som PC, Brandwei-Gensler MS. Anatomy and pathology of the salivary glands. In: Som PC, Curtin HD, eds. *Head and neck imaging*. St Louis: Elsevier, 2011;1950.
8. Terraz S, Poletti PA, Dulguerov P, et al. How reliable is sonography in the assessment of sialolithiasis? *AJR Am J Roentgenol* 2013;201:W104-W109.
9. Avrahami E, Englender M, Chen E, et al. CT of submandibular gland sialolithiasis. *Neuroradiology* 1996;38:287-290.
10. Tivers MS, Hotston AM. Surgical treatment of a parotid duct sialolith in a Bulldog. *Vet Rec* 2007;161:271-272.